Equilibrium Configurations and Capillary Interactions of Janus Dumbbells and Spherocylinders at Fluid-Fluid Interfaces

SUPPLEMENTARY INFORMATION

Carmine Anzivino,[1,*] Fuqiang Chang,[2] Giuseppe Soligno,[3]
René van Roij,[4] Willem K. Kegel,[2] and Marjolein Dijkstra[1,†]

[1] *Soft Condensed Matter, Debye Institute for Nanomaterial Science, Utrecht University, Princetonplein 1, Utrecht 3584 CC, The Netherlands*
[2] *Van 't Hoff Laboratory for Physical and Colloidal Chemistry, Debye Institute for Nanomaterial Science, Utrecht University, Padualaan 8, Utrecht 3584 CH, The Netherlands*
[3] *Condensed Matter and Interfaces, Debye Institute for Nanomaterial Science, Utrecht University, Princetonplein 1, Utrecht 3584 CC, The Netherlands*
[4] *Institute for Theoretical Physics, Center for Extreme Matter and Emergent Phenomena, Utrecht University, Princetonplein 5, Utrecht 3584 CC, The Netherlands*

(Dated: January 26, 2019)

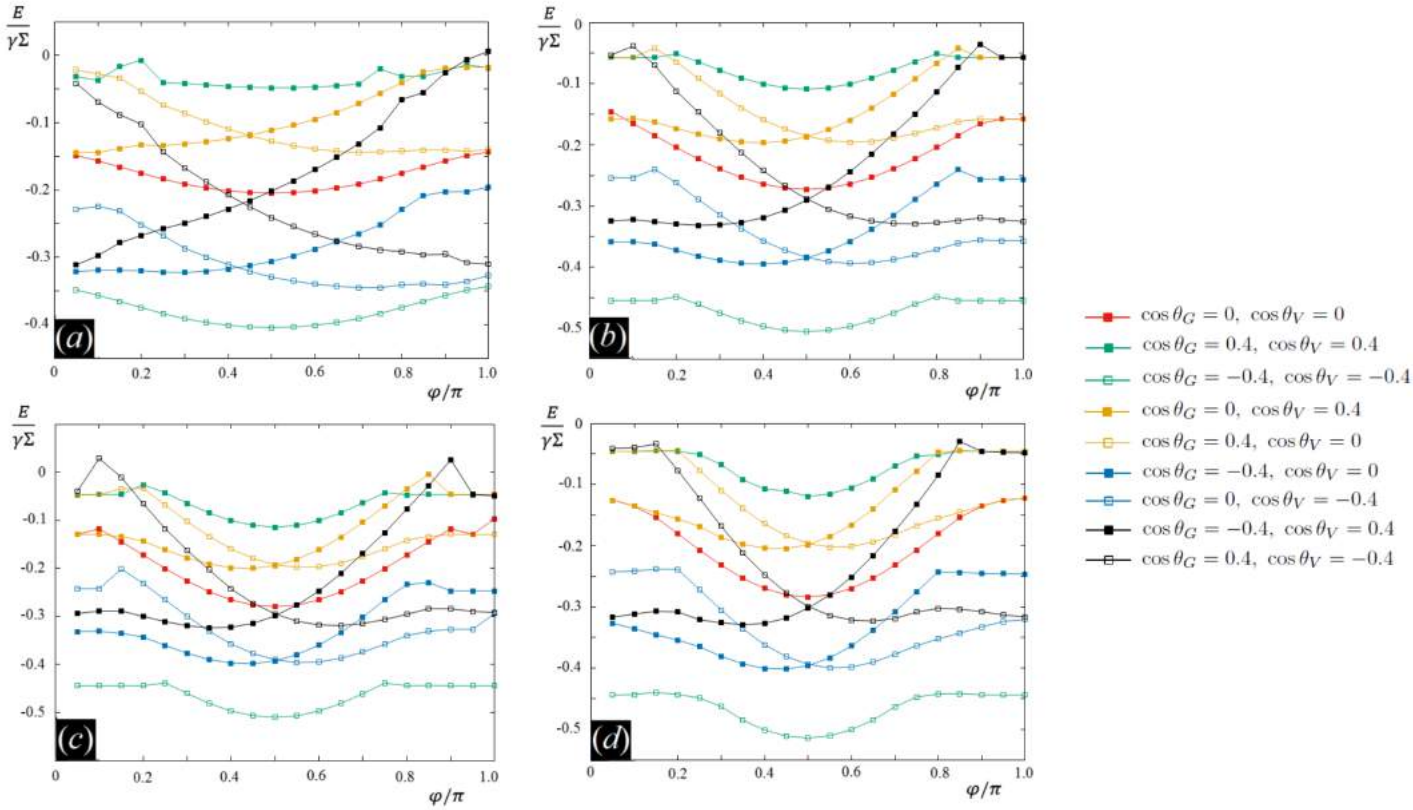

FIG. S1: Adsorption energy E (Eq. (2) of the main paper) for all the particles shapes considered in this paper (see Fig. 2 of the main paper) as a function of the polar angle φ at fixed combinations of the contact angles θ_G and θ_V. Here E is plotted in units of $\Sigma\gamma$ with γ the fluid-fluid surface tension and Σ the surface area of the particles. Observe that, as in Ref. [1], in our case E is already minimized with respect to the particle height z.

*Electronic mail: c.anzivino@uu.nl
†Electronic mail: m.dijkstra@uu.nl

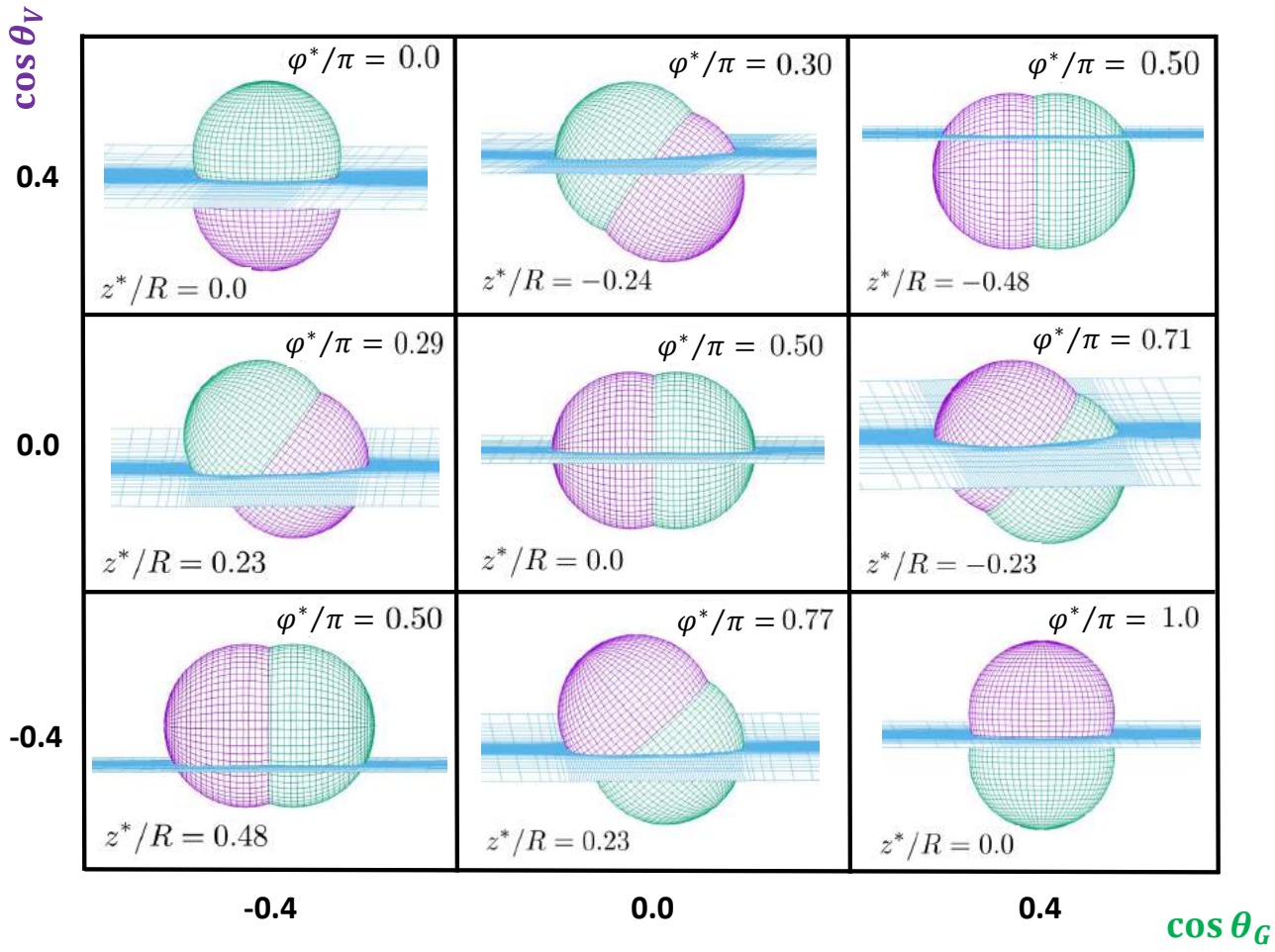

FIG. S2: 3D views of the equilibrium configurations of a Janus dumbbell (shape (a) in Fig. 2 of the main paper) adsorbed at a fluid-fluid interface, with varying contact angles θ_G and θ_V. The graph is symmetric with respect to the diagonal corresponding to the case of a homogeneous (non-Janus) dumbbell, i.e. $\theta_G = \theta_V$. In all the cases we do not observe any interfacial deformation.

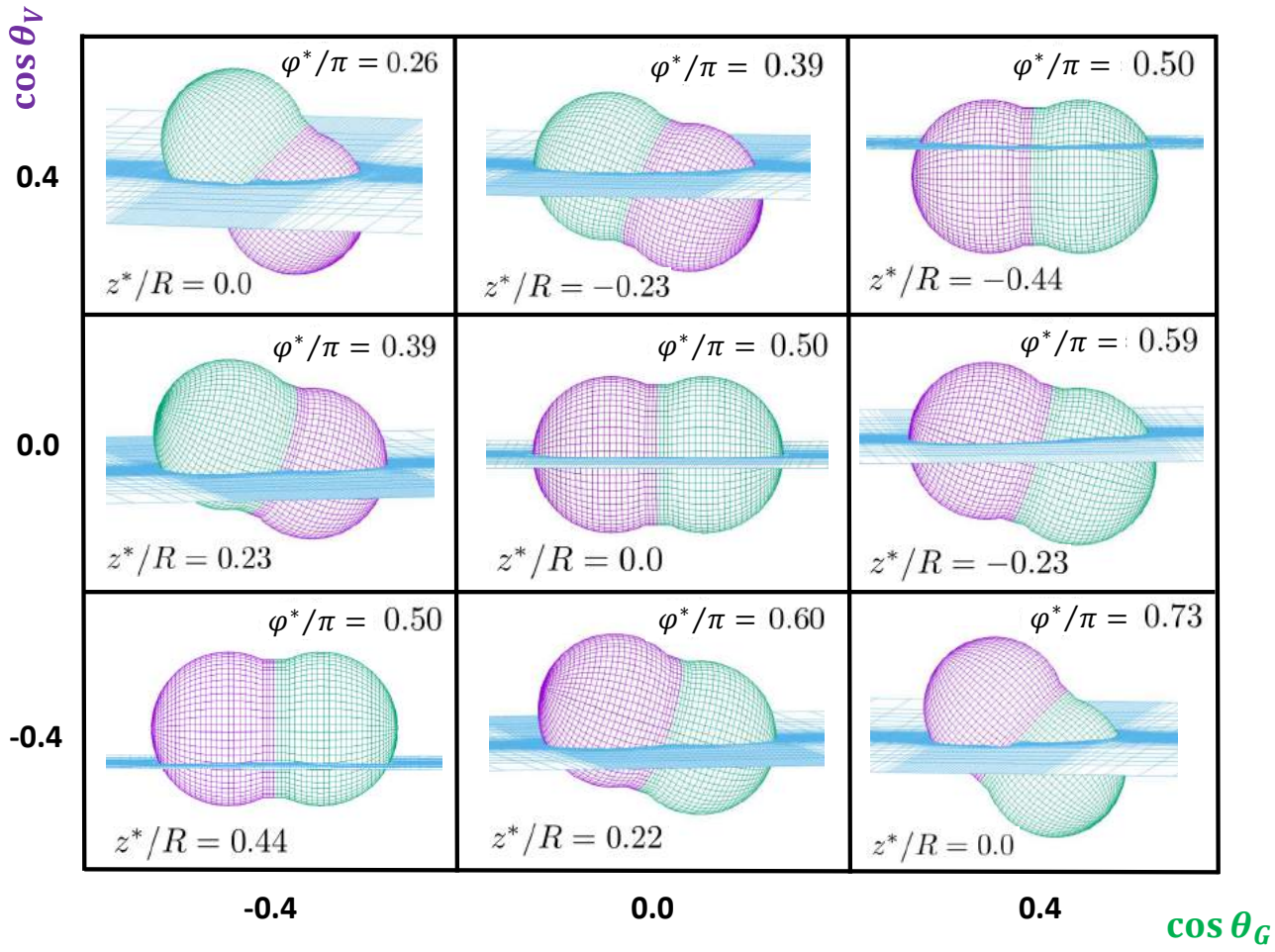

FIG. S3: 3D views of the equilibrium configurations of a Janus elongated dumbbell (shape (*b*) in Fig. 2 of the main paper) adsorbed at a fluid-fluid interface, with varying contact angles θ_G and θ_V. The graph is symmetric with respect to the diagonal corresponding to the cases of a homogeneous (non-Janus) dumbbell, i.e. $\theta_G = \theta_V$. When $\cos\theta_G = \cos\theta_V = 0$, $\varphi^*/\pi = 0.5$, $z^* = 0$, no interfacial deformations are induced in the fluid-fluid interface shape. For $\cos\theta_G = \cos\theta_V = \pm 0.4$, $\varphi^*/\pi = 0.5$, $z^*/R = \mp 0.44$, the induced interfacial deformation fields are flat as expected [2]. In all the off-diagonal cases, the deformation field is dominated by the hexapolar mode, whose intensity is proportional to $|\cos\theta_G - \cos\theta_V|$. This is shown in detail in Section IIIB of the main paper.

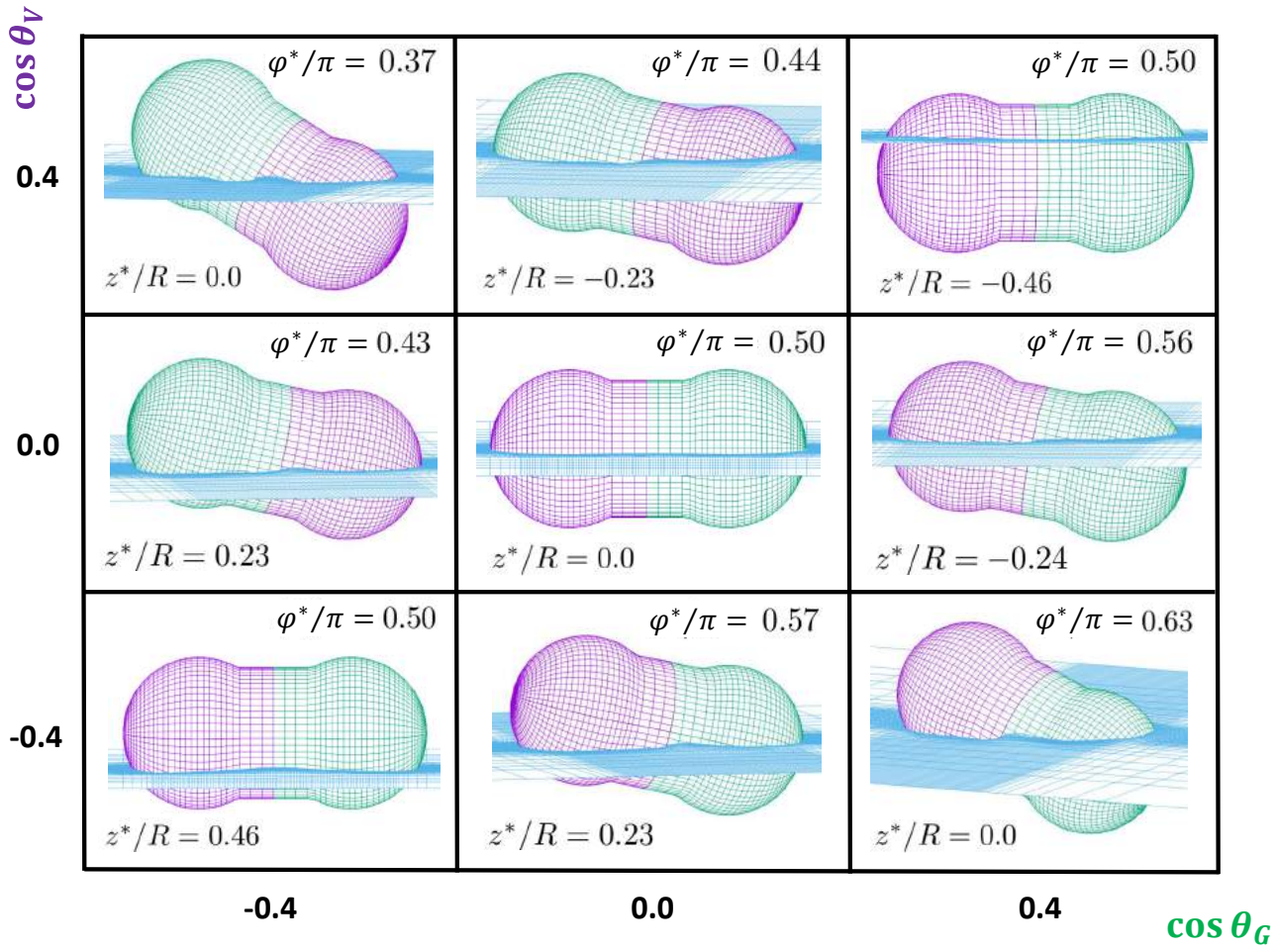

FIG. S4: 3D views of the equilibrium configurations of a Janus elongated dumbbell (shape (c) in Fig. 2 of the main paper) adsorbed at a fluid-fluid interface, with varying contact angles θ_G and θ_V. The graph is symmetric with respect to the diagonal corresponding to the cases of a homogeneous (non-Janus) dumbbell, i.e. $\theta_G = \theta_V$. When $\cos\theta_G = \cos\theta_V = 0$, $\varphi^*/\pi = 0.5$, $z^* = 0$, no interfacial deformations are induced in the fluid-fluid interface shape. For $\cos\theta_G = \cos\theta_V = \pm 0.4$, $\varphi^*/\pi = 0.5$, $z^*/R = \mp 0.46$, the induced interfacial deformation fields are flat as expected [2]. In all the off-diagonal cases, the deformation field is dominated by the hexapolar mode, whose intensity is proportional to $|\cos\theta_G - \cos\theta_V|$. This is shown in detail in Section IIIB of the main paper.

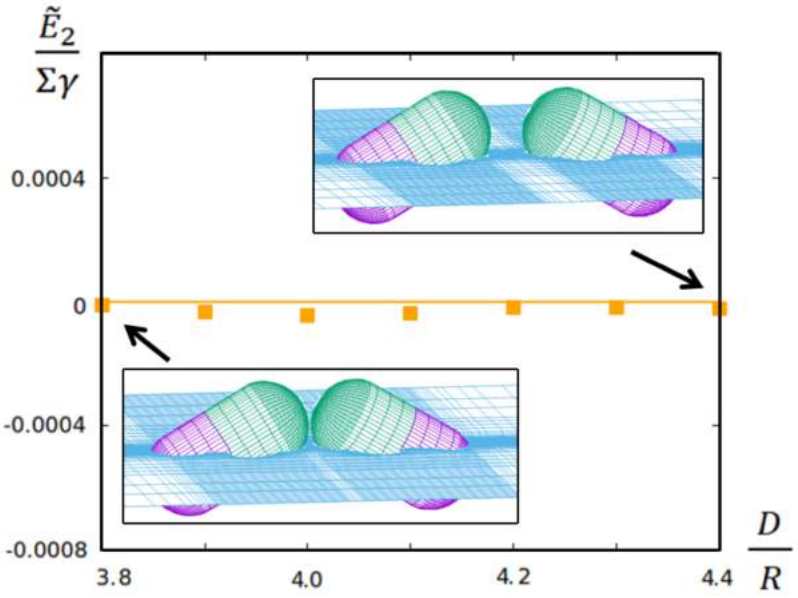

FIG. S5: Interaction energy per particle $\tilde{E}_2/\Sigma\gamma$ (Eq. (4) of the main paper) of two Janus spherocylinders, adsorbed in their equilibrium configuration, as a function of the distance D between their centers of mass. The total surface area is denoted as Σ and the fluid-fluid surface tension is γ. The contact angles of the Janus spherocylinders are given by $\cos\ \theta_G = -0.4$ (in green) and $\cos\ \theta_V = 0.4$ (in violet). We do not observe any tip-tip interaction between the spherocylinders.

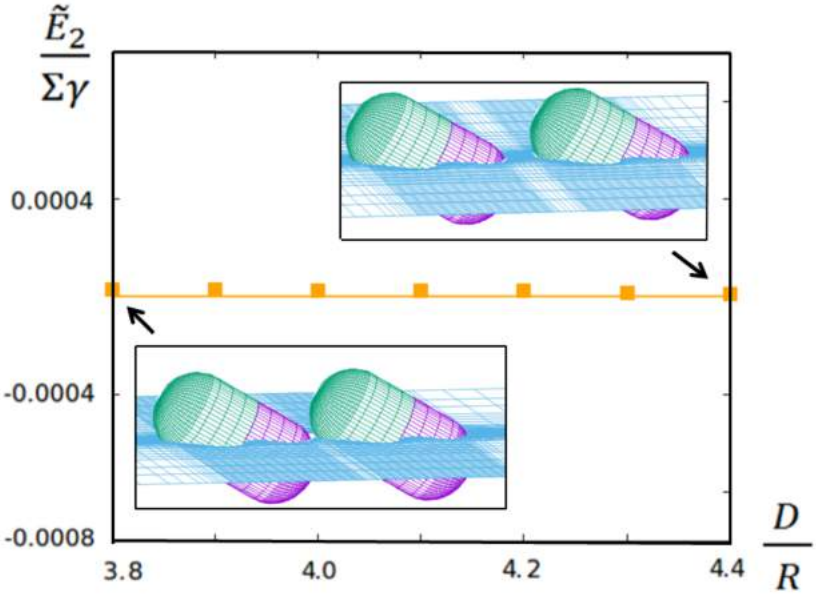

FIG. S6: Interaction energy per particle $\tilde{E}_2/\Sigma\gamma$ (Eq. (4) of the main paper) of two Janus spherocylinders, adsorbed in their equilibrium configuration, as a function of the distance D between their centers of mass. The total surface area is denoted as Σ and the fluid-fluid surface tension is γ. The contact angles of the Janus spherocylinders are given by $\cos\ \theta_G = -0.4$ (in green) and $\cos\ \theta_V = 0.4$ (in violet). We do not observe any tip-tip interaction between the spherocylinders.

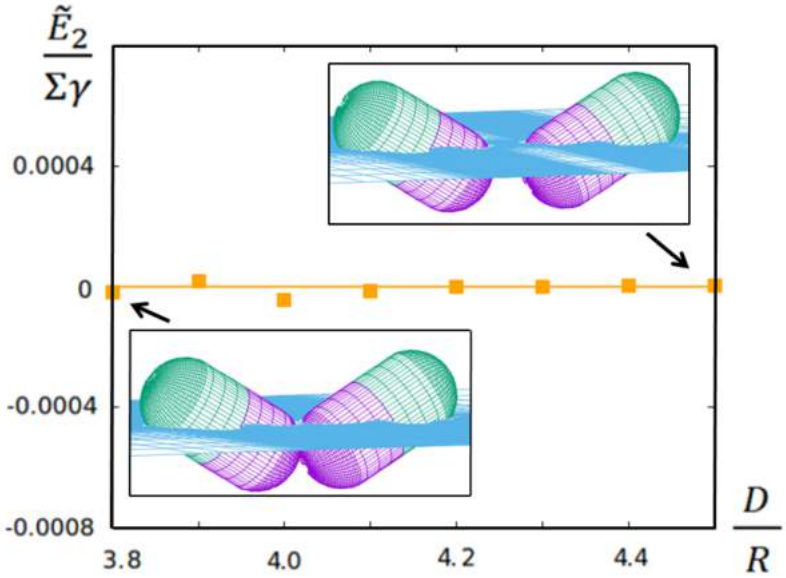

FIG. S7: Interaction energy per particle $\tilde{E}_2/\Sigma\gamma$ (Eq. (4) of the main paper) of two Janus spherocylinders, adsorbed in their equilibrium configuration, as a function of the distance D between their centers of mass. The total surface area is denoted as Σ and the fluid-fluid surface tension is γ. The contact angles of the Janus spherocylinders are given by $\cos\ \theta_G = -0.4$ (in green) and $\cos\ \theta_V = 0.4$ (in violet). We do not observe any tip-tip interaction between the spherocylinders.

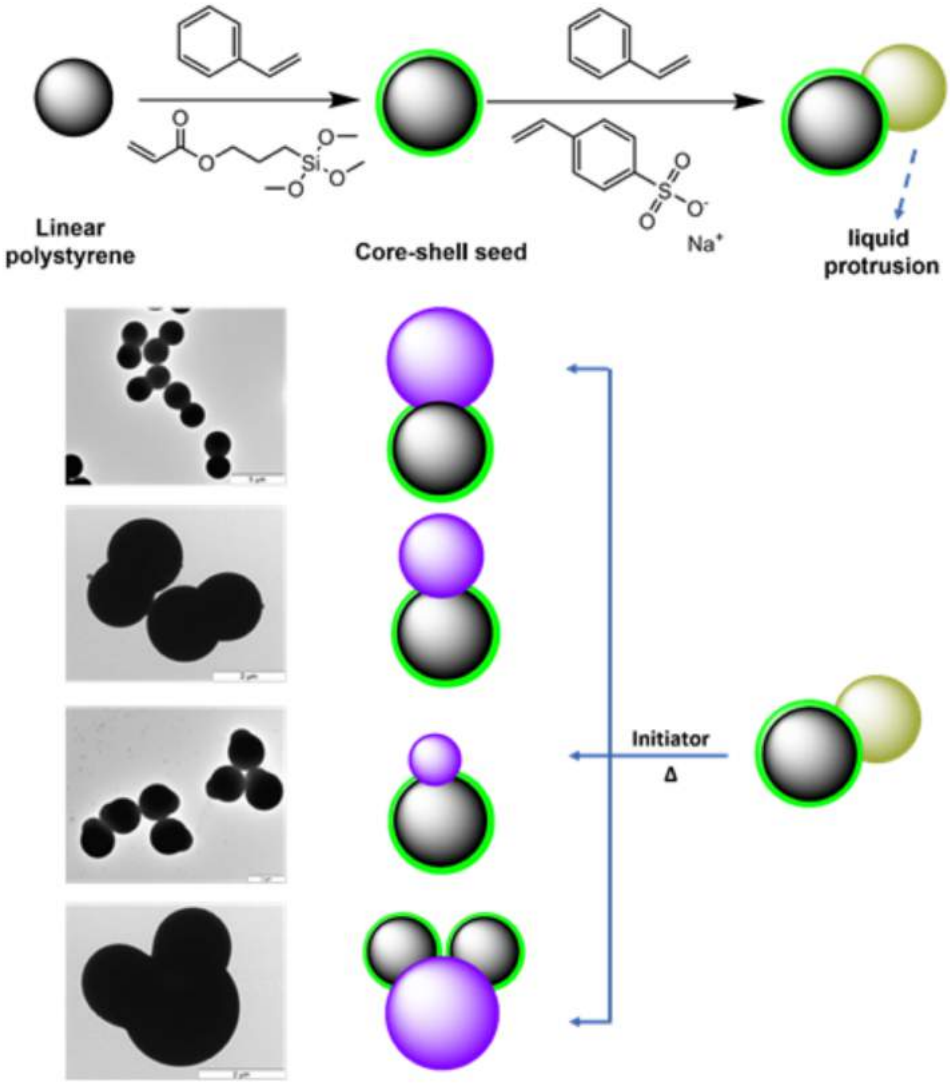

FIG. S8: Schematic illustration of the dumbbell formation via the two-step dispersion modification. Dumbbells with different size ratio or even trimers with two seeded lobes could be achieved via varying the swelling ratio and swelling time.

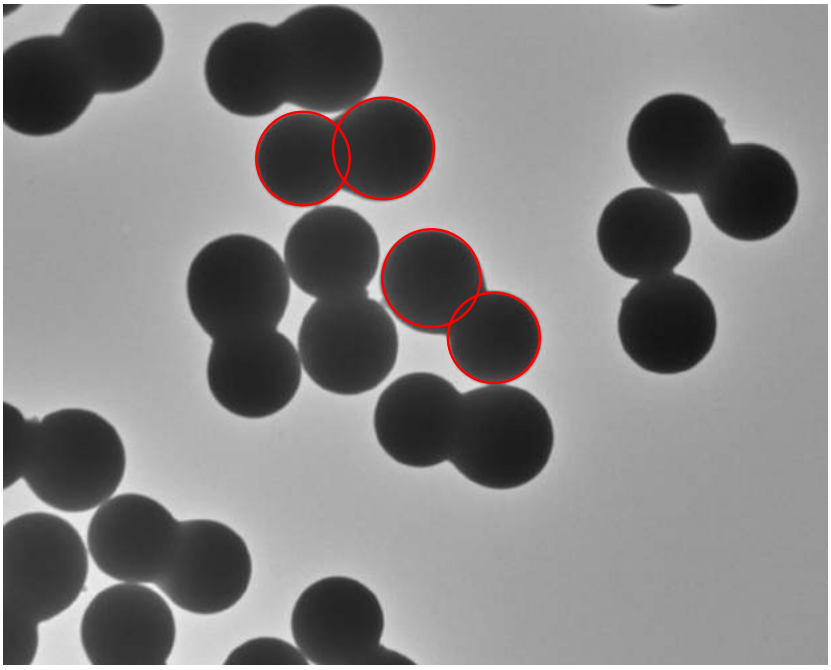

FIG. S9: Trasmission electron microscope images of symmetric Janus dumbbells. Their shape can best be compared to the dumbbells of Figs. 2(b) and 2(c) in the main paper, i.e. dumbbells consist of smoothly joined, interpenetrating or touching spheres.

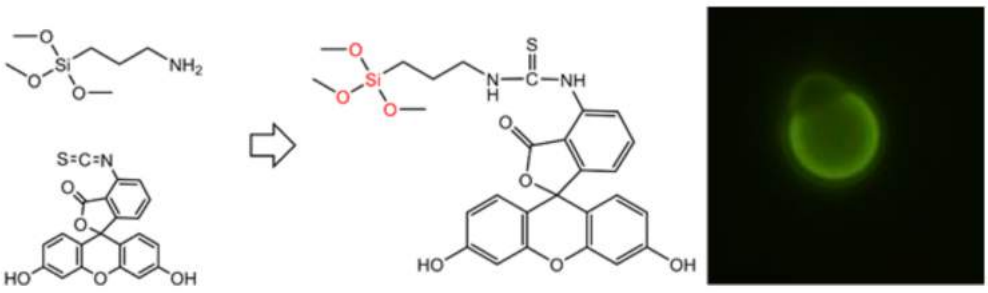

FIG. S10: Dye molecules can be selectively bond to the PS-TM SPA core shell seed lobes which contain plenty of silanol groups. To label the dumbbells with fluorescent dye, the dye molecules (fluorescein-isothiocyanate) first need to react with a coupling agent, in our case 3-aminopropyltriethoxysilane (APS), which acts as a bridge between dye and TPM molecules. The preparation of the dye solution is by adding 0.01428 mmol fluorescein-isothiocyanate and 3.61 mmol APS to 10 mL ethanol. This dye stock solution was stirred overnight in the dark and then stored afterwards in a refrigerator (4 °C). The seeded lobe of the dumbbells was labelled by mixing 50 L APS-FITC (or APS-RITC) with 0.5 mL dispersion in water, and the mixture was reacted for 20 hours on a roller table at 60 rpm under protection from light.

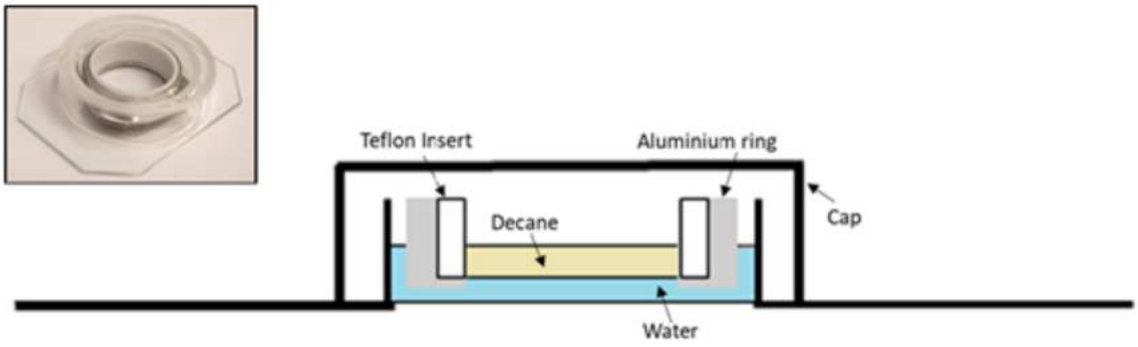

FIG. S11: A monolayer containing dumbbell particles was prepared by spreading the dispersion onto a fluid-fluid interface. About μL of dispersion with a particle content of 1.5 wt% was used with a mixture of isopropyl alcohol (IPA) and water (7:3 v/v) as spreading solvent. Aluminium oxide (basic) purified decane was used as the oil phase and MilliQ water as a sub-phase. Glass cell consisting of an aluminium outer ring and a Teflon inner ring connected with glass spacers was used to ensure a pinned liquid interface [3–5]. The dumbbell particle suspension in the mixture of IPA-water was injected at the interface using a micro syringe. The tip of the syringe was slightly under the interface when we inject the particles to the interface thereby ensuring that all particles were brought to the interface via spreading of the solvent. Otherwise the dumbbells might form aggregates in the oil phase before reaching the liquid-liquid interface. In the experimental cell, the aluminum ring and the Teflon ring ensure the interface, and the connection between the inner aluminum ring and the outer glass ring allows us to tune the height of the water phase and to get a flat interface.

[1] G. Soligno, M. Dijkstra and R. van Roij, Soft Matter **14**, 42 (2018).
[2] T.G. Anjali and M.G. Basavaray, J. Colloid. Interface Sci. **478**, 63-71 (2016).
[3] B.J. Park, J. Vermant and E.M. Furst, Soft Matter **6**, 5327-5333 (2010).
[4] B.J. Park and E.M. Furst, Soft Matter **7**, 7676-7682 (2011).
[5] N.A. Elbers, J.E.S. van der Hoeven, D.A.M. de Winter, C.T.W.M. Schneijdenberg, M.N. van der Linden, L. Filion and A. van Blaaderen, Soft Matter **12**, 7265-7272 (2016).